INL/CON-13-28052
PREPRINT

Pyroprocessing Of Oxidized Sodium-Bonded Fast Reactor Fuel – An Experimental Study of Treatment Options for Degraded EBR-II Fuel

GLOBAL 2013

S. D. Herrmann
L. A. Wurth
N. J. Gese

September 2013

The INL is a
U.S. Department of Energy
National Laboratory
operated by
Battelle Energy Alliance

PYROPROCESSING OF OXIDIZED SODIUM-BONDED FAST REACTOR FUEL – AN EXPERIMENTAL STUDY OF TREATMENT OPTIONS FOR DEGRADED EBR-II FUEL

S. D. Herrmann,[a] L. A. Wurth,[b] N. J. Gese[a]

[a]*Separations Department, Idaho National Laboratory, P.O. Box 1625, Idaho Falls, Idaho, 83415, USA, steven.herrmann@inl.gov*
[b]*Zinc Air Inc., 5314-A US Hwy 2 West, Columbia Falls, MT, 59912, USA*

An experimental study was conducted to assess pyrochemical treatment options for degraded EBR-II fuel. As oxidized material, the degraded fuel would need to be converted back to metal to enable electrorefining within an existing electrometallurgical treatment process. A lithium-based electrolytic reduction process was studied to assess the efficacy of converting oxide materials to metal with a particular focus on the impact of zirconium oxide and sodium oxide on this process. Bench-scale electrolytic reduction experiments were performed in LiCl-Li_2O at 650 °C with combinations of manganese oxide (used as a surrogate for uranium oxide), zirconium oxide, and sodium oxide. The experimental study illustrated how zirconium oxide and sodium oxide present different challenges to a lithium-based electrolytic reduction system for conversion of select metal oxides to metal.

I. INTRODUCTION

An engineering-scale electrometallurgical treatment (EMT) process has been operating at Idaho National Laboratory (INL) since 1996 to treat 25 metric tons of heavy metal from sodium-bonded uranium and uranium alloy blanket and driver fuels that have accumulated from Experimental Breeder Reactor (EBR-II) operations over a 30-year lifetime, i.e., from 1964 – 1994.[1] At the heart of the EMT process is an electrorefiner containing a molten salt pool of LiCl-KCl-UCl_3 at 500 °C. Chopped sodium-bonded metal fuel segments are loaded into a permeable steel anode basket and immersed in molten electrorefining salt along with a solid metal cathode rod. A controlled current is applied to dissolve (oxidize) uranium metal from the basket into the salt pool, while uranium ions in the salt are simultaneously reduced to metal and deposited on the cathode rod. The bond sodium and those fission products that form more stable chlorides than uranium trichloride (i.e., alkali, alkaline earth, lanthanide, and transuranic elements) partition from the fuel to the salt pool at the expense of UCl_3. Those fission products and uranium alloying agent(s) that are nobler than UCl_3 (i.e., zirconium, molybdenum, ruthenium, technetium palladium, and rhodium) remain as metal with the steel cladding hulls in the anode baskets. The cladding hulls, containing noble metal fission products and alloying agent(s), are subsequently removed and processed into a consolidated metal waste form. Stable fission product chlorides are allowed to accumulate in the salt pool, but will ultimately be processed into a ceramic waste form.[2]

In the course of retrieving spent EBR-II fuel for treatment, minor portions of the driver fuel have been found in a degraded state due to cladding breaches and air exposure, resulting in partial to complete oxidation of these sodium-bonded uranium alloy fuels. The degraded uranium alloys are primarily U-10Zr, but also include U-5(Mo/Ru/Rh/Pd/Zr/Nb), and U-Pu-Zr. As oxidized material, these degraded EBR-II driver fuels would need to be converted back to metal to enable electrorefining within the prescribed EMT process.

A lithium-based electrolytic reduction process has been developed by researchers at Argonne National Laboratory to convert uranium oxide to metal as a head-end step to uranium electrorefining,[3] enabling extension of the prescribed EMT process to spent nuclear oxide fuels. In this process, uranium oxide fuel particulate is loaded into a permeable steel cathode basket and immersed in a molten salt pool of LiCl – 1 wt% Li_2O at 650 °C. A controlled electric current reduces oxides in the cathode basket to metal, liberating its oxygen ions that are soluble in the molten salt. Dissolved oxygen ions in the salt are simultaneously oxidized at an anode to gas, which dissipates from the electrolytic reduction cell. Separation and recovery of uranium metal from spent light water reactor fuel via electrolytic reduction and electrorefining has been demonstrated at bench scale at INL.[4]

An experimental study was performed to assess application of the prescribed lithium-based electrolytic reduction system to degraded EBR-II driver fuel. Degraded EBR-II fuel contains substantial quantities of zirconium oxide and sodium oxide, which are not present

to any appreciable extent in typical spent nuclear oxide fuel. Thus, the impacts of zirconium oxide and sodium oxide on a lithium-based electrolytic reduction process were the primary focus of this study. Given a focus on zirconium oxide and sodium oxide behavior in the prescribed reduction process, as opposed to uranium oxide conversion to metal, this study used manganese oxide as a surrogate for uranium oxide to eliminate the need for radiological controls.

II. EXPERIMENT

II.A. Approach

The approach for this study was to perform a series of three electrolytic reduction experiments using a common initial loading of LiCl – 1 wt% Li_2O at 650 °C and introducing zirconium oxide and sodium oxide accumulatively in separate runs. Accordingly, the first run was performed with MnO as the cathode material to verify the suitability of this material as a surrogate for UO_2 and to establish a baseline for the subsequent runs. The second run was performed with a blend of MnO and ZrO_2 particulate with the respective oxides proportioned on a molar basis to that expected in an oxidized U-10Zr fuel. The third run was performed with the same blend of MnO and ZrO_2 as the second run, but after adding 50 g of sodium oxide to the LiCl – 1 wt% Li_2O electrolyte. This addition simulated the expected accumulation of sodium oxide in the salt pool from repeated treatment of degraded EBR-II fuel without exceeding the estimated solubility limit of sodium oxide in the base electrolyte. The three electrolytic reduction experiments in this study are summarized in Table I.

TABLE I. Test Matrix

Run No.	Cathode Material	Molten Salt Electrolyte
1	MnO	LiCl – 1 wt% Li_2O
2	MnO-ZrO_2	LiCl – 1 wt% Li_2O
3	MnO-ZrO_2	LiCl –1 wt% Li_2O + 50 g Na_2O

The salt level was measured and salt samples were taken before and after electrolytic reduction runs 1 and 2. The salt samples were analyzed for lithium oxide concentration. Lithium chloride and lithium oxide were added, as necessary, after runs 1 and 2 to restore the salt level and lithium oxide concentrations in the salt to that established at the beginning of run 1.

Cyclic voltammetry (typically at 50 mA/sec) was performed periodically in the study to identify reaction potentials on stainless steel and platinum working electrodes in the salt and with the reactive materials loaded in each of the 3 cathode baskets.

II.B. Equipment

The series of electrolytic reduction runs was performed in a molten salt furnace that is installed in an argon atmosphere glovebox at INL. A sectional view of the furnace is shown in Fig. 1.

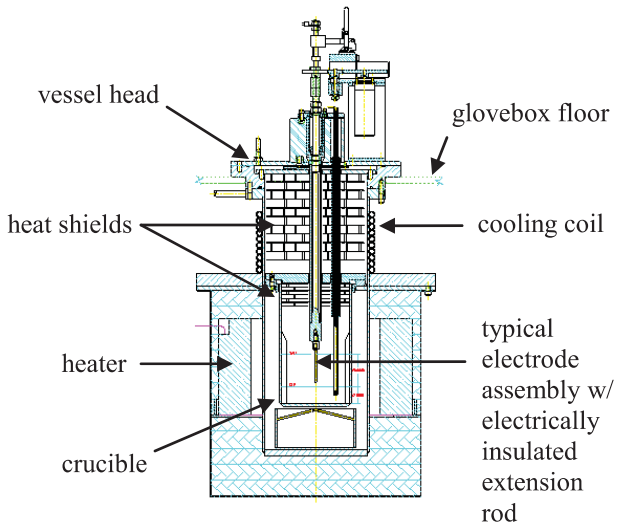

Fig. 1. Sectional view of molten salt furnace.

The molten salt furnace consists of a cylindrical steel thermal well that is connected to a flanged penetration in a glovebox floor. The lower end of the thermal well is enveloped by an insulated resistance-heated furnace assembly to heat a steel crucible that is suspended inside the thermal well. Coolant is circulated through a copper tubing coil around the upper thermal well to limit conductive heat transfer into the glovebox floor. Head shields above the crucible limit heat transfer into the glovebox atmosphere.

The suspended steel crucible was lined with an MgO crucible (Ozark Technical Ceramics) to contain the molten salt pool. The heat shields and vessel head are fitted with four ports for thermocouple and electrode positioning, i.e., one 2.2-cm diameter center port and three 1.6-cm diameter perimeter ports 120 degrees apart on a 3.2-cm radius.

The cathode baskets consisted of a 1.9-cm diameter open top and closed bottom stainless steel tube. The lower end of the tube was perforated and wrapped with 325 x 325 stainless steel wire mesh. An electrically isolated stainless steel rod was suspended on center inside the tube and configured as the cathode to a potentiostat. Openings in the tube immediately above the perforated and mesh-wrapped region enabled filling of the basket with select cathode materials. A cathode basket assembly is shown in Fig. 2.

The anode for all three runs consisted of 1-mm diameter Pt wire (99.95%, Alfa Aesar) that was wound

into a spiral approximately 0.6 cm diameter and 5 cm tall, creating a total surface area in contact with the salt of 10 cm^2. The Pt wire coil was connected to a stainless steel extension rod above the salt level to provide an electrical connection atop the vessel to a potentiostat.

A stainless steel sheathed thermocouple was positioned in the molten salt pool to monitor the salt temperature. A Ni/NiO reference was positioned in the salt pool to provide relative anode and cathode readings. Indeed, all anode and cathode potentials reported in this article are relative to the Ni/NiO reference electrode.

One mm diameter Pt and stainless steel wires were fitted to extension rods to serve as low surface area working electrodes for characterizing the salt via cyclic voltammetry. A spiral wound 1-mm diameter molybdenum wire was fitted to an extension rod to serve as a large surface area counter electrode for the same cyclic voltammetry runs. The working and counter electrodes are shown in Fig. 3. A BioLogic VSP potentiostat was used for the cyclic voltammetry and electrolytic reduction runs.

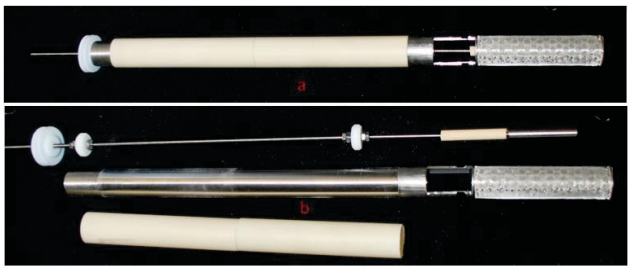

Fig. 2. Cathode basket asembly (a); basket, center conductor, and alumina sheath (b).

Fig. 3. Stainless steel and platinum wire working electrodes (top and bottom); molybdenum wire counter electrode (center).

An auto-titrator (Shott, TitroLine *easy*) was used to determine dissolved oxide concentrations in samples of the molten salt over the course of the series of electrolytic reduction runs.

II.C. Materials

The molten salt electrolyte was prepared from anhydrous LiCl (Aldrich-APL, 99.99%) and Li_2O (Alfa Aesar, 99.5%). Manganese (II) oxide, MnO (Alfa Aesar, 99.99%), and zirconium (IV) oxide, ZrO_2 (Alfa Aesar, 99.978%), particulates were sieved to a range of particle size greater than 0.045 mm but less than 1 mm prior to loading into the respective cathode baskets. Sodium oxide (Alfa Aesar) was dissolved into the molten salt electrolyte prior to commencing run 3.

III. TEST PERFORMANCE AND RESULTS

A molten salt electrolyte was prepared by adding 750 g of LiCl to an MgO crucible (10 cm diameter, 11 cm tall) inside of a steel crucible and heating it in MSF-II to 650 °C. A reference electrode and thermocouple were placed in perimeter ports. A total of 7.5 g of lithium oxide was added in two parts to the salt pool to create concentrations of 0.5 wt% and then 1.0 wt%. Cyclic voltammetry (CV) was performed before and after each lithium oxide addition, while alternating between stainless steel and platinum wire working electrodes. Cyclic voltammetry results for the stainless steel and platinum wire working electrodes are shown in Figs. 4 and 5, respectively.

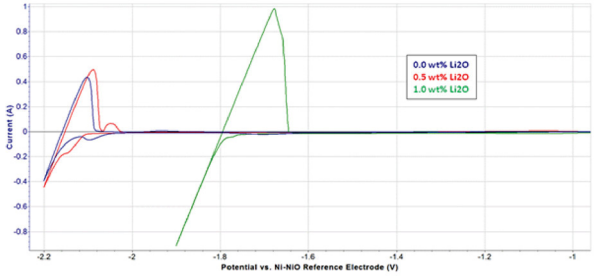

Fig. 4. Cyclic voltammetry on stainless steel wire prior to run 1 in LiCl and varying concentrations of Li_2O at 650 °C.

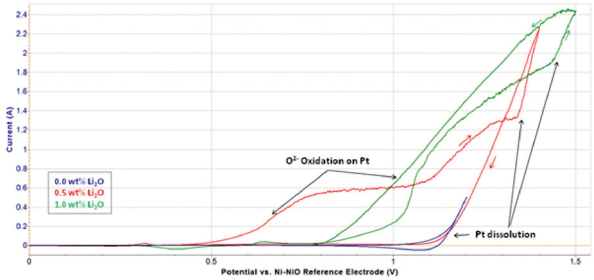

Fig. 5. Cyclic voltammetry on platinum wire prior to run 1 in LiCl and varying concentrations of Li_2O at 650 °C.

A pre-test salt sample was taken and titrated, yielding a lithium oxide concentration in the salt of 1.12 wt%. The first cathode basket assembly was loaded with 27.53 g of MnO and immersed in the salt. Cyclic voltammetry was performed on the first cathode basket, the results of which are shown in Fig. 6.

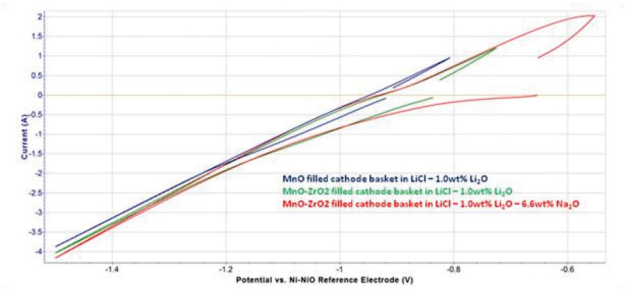

Fig. 6. Cyclic voltammetry on cathode material baskets in the prescribed electrolyte systems at 650 °C.

The MnO loaded cathode basket was allowed to soak in the salt for 16 hours, after which a salt sample was taken and titrated. The lithium oxide concentration in the salt sample was 1.09 wt%.

The platinum anode was immersed in the salt pool, and a controlled current of 3A was applied between the anode and the first fuel basket as shown in Fig. 7. The anode and cathode potentials were steady at +1.0 V and –1.5 V, respectively for the balance of the first day, after which the current was lowered to 50 mA for unattended overnight operations. The next day the current was restored to 3 A, and anode and cathode potentials returned to similar levels as those from the previous day. After 22 A-hrs of charge had been applied, the cathode potential began to lower. The current was consequently stepped down and then de-energized after nearly 26 A-hrs of charge was applied.

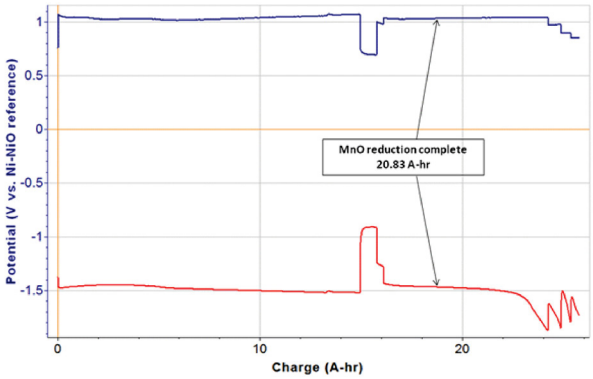

Fig. 7. Response plot for electrolytic reduction of MnO in LiCl – 1 wt% Li_2O at 650 °C (run 1).

The platinum anode and cathode basket from the first run were removed, and a salt sample was taken. Titration revealed a post-test lithium oxide concentration in the salt of 0.98 wt%.

The second basket assembly was loaded with a blend of MnO (17.94 g) and ZrO_2 (9.07 g) particulate and immersed in the salt pool. After soaking for 2 hrs, a salt sample was taken and titrated. The lithium oxide concentration in the salt after the 2-hr soak was 0.97 wt%. The same platinum anode was immersed in the salt, and cyclic voltammetry was performed on cathode basket 2. The CV response for cathode basket 2 was very similar to that from basket 1, as shown in Fig. 6.

A controlled current was applied across cathode basket 2 and the platinum anode, and the respective potentials were monitored as shown in Fig. 8. At 3 A the anode and cathode potentials responded similarly to those from the first run, i.e., approximately +1.0 V and -1.5 V, respectively. After 14 A-hrs of charge had been applied, the cathode potential began to lower rapidly. The current was then lowered to 50 mA for unattended overnight operations. The next day the current was raised to 2A, and the cathode potential settled at -2 V with the anode potential remaining at +1 V. After 35 A-hrs of charge had been applied with no significant change in anode or cathode potential, the current was stopped.

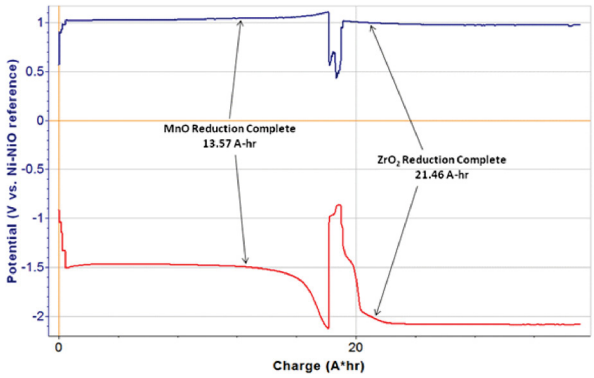

Fig. 8. Response plot for electrolytic reduction of MnO-ZrO_2 in LiCl – 1 wt% Li_2O at 650 °C (run 2).

The platinum anode and cathode basket 2 were removed from the salt pool, and a salt sample was taken. Titration revealed a lithium oxide concentration of 0.45 wt% in the salt after run 2. Lithium chloride and lithium oxide were then added to the salt pool to restore the salt level to initial conditions and the lithium oxide concentration to 1 wt%. Indeed, a salt sample was taken and titrated, yielding a lithium oxide concentration of 0.96 wt% prior to starting run 3.

Fifty grams of sodium oxide was added to the salt pool via a permeable (i.e., wire mesh wrapped) closed end stainless steel tube to ensure all of the sodium oxide particulate dissolved into the salt pool. The absence of sodium oxide particulate in the permeable tube after the addition showed that the solubility limit of sodium oxide in LiCl – 1 wt% Li_2O at 650 °C had not been reached.

Cyclic voltammetry was performed on stainless steel and platinum wire working electrodes in the prepared LiCl – 1 wt% Li_2O – 6.2 wt% Na_2O electrolyte, the responses of which are shown in Figs. 9 and 10, respectively, along with those from the same working electrodes in LiCl – 1 wt% Li_2O at 650 °C prior to run 1.

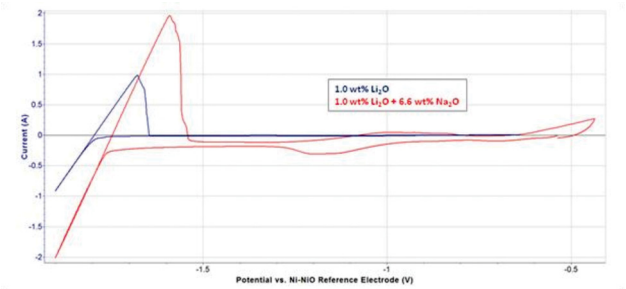

Fig. 9. Cyclic voltammetry on stainless steel wire prior to runs 1 and 3 in LiCl and varying concentrations of Li_2O and Na_2O at 650 °C.

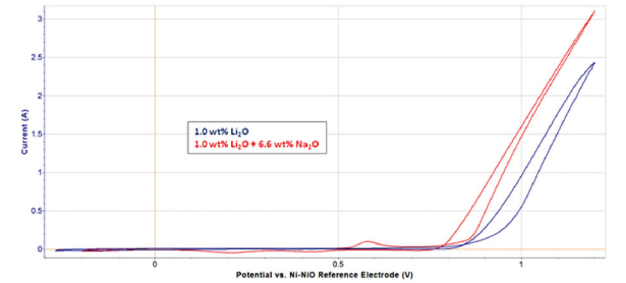

Fig. 10. Cyclic voltammetry on platinum wire prior to runs 1 and 3 in LiCl and varying concentrations of Li_2O and Na_2O at 650 °C.

The third basket assembly was loaded the same as basket assembly 2, i.e., with a blend of 17.93 g of MnO and 9.07 g of ZrO_2 particulate. Cathode basket 3 was immersed in the salt pool, and cyclic voltammetry was performed. The CV response for cathode basket 3 was similar to those from baskets 1 and 2, as shown in Fig. 6.

A controlled current was applied across cathode basket 3 and the same platinum anode from runs 1 and 2, and the respective potentials were monitored as shown in Fig. 11. At 3 A the anode and cathode potentials responded similarly to those from the first run, i.e., approximately +1.0 V and -1.5 V, respectively. After 16 A-hrs of charge had been applied the current was lowered to 50 mA for unattended overnight operations. The next day the current was restored to 3 A, and anode and cathode potentials returned to similar levels as those from the previous day. After 20 A-hrs of charge had been applied, the cathode potential began to drift lower and the anode potential higher, but not to any appreciable extent. After 42 A-hrs of charge had been applied, the current was stopped. Cathode basket 3, the platinum anode, the reference electrode, and the thermocouple were removed from the salt pool, and the molten salt furnace was de-energized.

Each of the cathode basket assemblies was cut and crushed to dislodged surrogate fuel material for analysis. Samples from each post-test cathode basket were separated into metal and oxide phases by contacting each sample with elemental bromine in an ethyl acetate medium. The bromine dissolved the metals in a sample, leaving the oxide compound(s) in an insoluble solid phase. The insoluble solids were separated from the ethyl acetate solution by filtration and additional ethyl acetate washing. Once separated, each of the metal and oxide phases was analyzed via Inductively Coupled Plasma – Mass Spectroscopy (ICP-MS). The fraction of material in the metal phase from the series of three electrolytic reduction runs is shown in Table II.

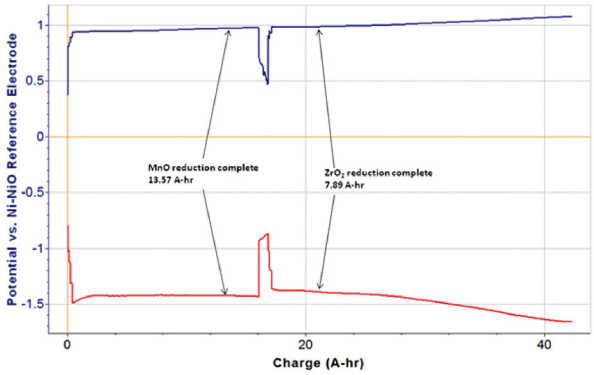

Fig. 11. Response plot for electrolytic reduction of MnO-ZrO_2 in LiCl – 1 wt% Li_2O – 6.2 wt% Na_2O at 650 °C (run 3).

Table II. Fraction of Cathode Material in Metal Phase Following Electrolytic Reduction Runs

Run No.	Mn	Zr
1	94%	n/a
2	71%	8.5%
3	76%	2.4%

The technique to separate metal and oxide phases from an electrolytically reduced sample was based on previous work by others for separation of uranium metal and uranium oxide.[5,6] The technique should apply to manganese and zirconium metal and oxide. However, no exhaustive analysis campaign was performed in this study to validate this separation technique for the various manganese and zirconium oxide phases against their respective metals. Thus, the results in Table II are considered reasonable approximations.

IV. DISCUSSION

The ability of a lithium-based electrolytic reduction process to convert uranium oxide to uranium metal is based on the thermodynamics of the system. Table III shows the Gibbs free energies of formation and standard decomposition potentials for uranium oxide in a LiCl-Li_2O system at 650 °C along with other compounds included or considered in this study. Accordingly, uranium oxide may be converted to metal directly by applying a nominal decomposition potential in the

prescribed system in excess of 2.40 V, or indirectly by forming lithium metal (with a decomposition potential of 2.47 V) and allowing it to chemically reduce UO_2 via the following reaction mechanism.

$$4\ Li + UO_2 \rightarrow U + 2\ Li_2O,\ \Delta G_f = -26.18\ kJ/mol \quad (1)$$

Table III. Gibbs Free Energies of Formation and Standard Decomposition Potentials at 650 °C.[7]

Compound	ΔG_f (kJ/mol O or Cl)	E° (V)
Na_2O	-288.24	1.49
MnO	-317.21	1.64
$NaMnO_4$	-329.93	1.71
Na_2ZrO_3	-461.30	2.39
ZrO_2	-461.95	2.39
UO_2	-462.65	2.40
Li_2O	-475.73	2.47
Li_2ZrO_3	-488.49	2.53
NaCl	-325.60	3.37
LiCl	-333.71	3.46

The selection of MnO as a surrogate is based on its relative ease of reduction compared to UO_2 and its lack of mixed oxide formations that could interfere in the subject study. While $NaMnO_4$ may form in a system containing MnO and Na_2O, the manganese in the mixed oxide should still be converted to metal with the reducing conditions established in this study. No thermodynamic information was available for the possible formation of $LiMnO_4$. However, the substantial reduction of MnO in run 1 suggests that $LiMnO_4$ interference was not an issue.

The addition of ZrO_2 to a LiCl – 1 wt% Li_2O reduction system enables the formation of Li_2ZrO_3 that is more stable than Li_2O (see Table III), suggesting that a lithium-based electrolytic reduction system may be insufficient to substantially reduce zirconium oxide to metal. However, the stability of Li_2ZrO_3 in a reducing system is a function of the oxygen ion activity in the molten salt electrolyte, i.e., the lower the oxygen ion activity in the salt, the more likely Li_2ZrO_3 may be reduced to metal. However, analysis of the cathode product in runs 2 and 3 showed that zirconium remained substantially in the oxide phase. Indeed, the fraction of zirconium in the oxide phase was higher in the product from run 3 which was in contact with a molten salt electrolyte containing a higher oxygen ion activity. The inability to substantially reduce ZrO_2 in a LiCl-Li_2O system is consistent with results by others.[8]

While the addition of sodium oxide to the subject system could lead to mixed oxide formations with manganese and zirconium, such were not anticipated under the reducing conditions generated in this study. A possible impact of sodium oxide in this study is competition for reduction between sodium and lithium ions at the cathode. If sodium metal were generated at the cathode and not consumed or otherwise bound, it could enter the salt phase and introduce a parasitic reaction by its cyclic oxidation at the anode and reduction at the cathode.

The first run in this study showed typical initial conditions for a LiCl – 1 wt% Li_2O system with Li reduction below -1.8 V, oxygen ion oxidation above +0.8 V, and platinum dissolution above +1.1 V. Cyclic voltammetry on the first cathode basket showed MnO reduction below -0.9 V. The theoretical charge for the material loaded into basket 1, along with those for runs 2 and 3, are shown in Table IV. The electrolytic reduction response for the first run exhibited stable anode and cathode potentials for the theoretical charge of MnO (i.e., 20.81 A-hr). After 22 A-hrs the cathode potential lowered rapidly, which is consistent with the complete reduction of MnO and the subsequent transition to lithium metal formation at the cathode. The post-test analysis of the cathode material showed nearly complete reduction of manganese to metal.

Table IV. Cathode Basket Material Loadings and Theoretical Charge

Run No.	Material	Mass (g)	Charge (A-hr)
1	MnO	27.53	20.81
2	MnO	17.94	13.55
	ZrO_2	9.07	7.89
	total	27.01	21.44
3	MnO	17.93	13.55
	ZrO_2	9.07	7.89
	total	27.00	21.44

The electrolytic reduction response for the second run exhibited stable anode and cathode potentials until after the theoretical charge of MnO was applied (i.e., 13.55 A-hr), when the cathode potential lowered rapidly. The overnight current suppression and next-day return to 2A caused the cathode potential to stabilize at a level where lithium metal should form. Run 3 was terminated after 35 A-hrs were applied, which is substantially beyond the theoretical charge of 21.44 A-hr for the MnO-ZrO_2 basket loading. Sufficient time at potential was applied to reduce zirconium oxide, yet post-test analysis showed that only 8.5% of zirconium in the cathode product was present in the metal phase. The lithium oxide concentration in the salt pool lowered over the course of run 2 from 0.98 to 0.45 wt%, which accounts for about half of the excess charge (i.e., half of 35 minus 21.44 A-hrs, or 7 A-hrs). The balance of the excess charge could likely have been a parasitic and cyclic reaction of lithium metal oxidation at the anode and reduction at the cathode.

The only parameter change in run 3 versus run 2 was the up-front addition of sodium oxide to the molten salt electrolyte. Yet, the electrolytic reduction response for

run 3 behaved differently. Specifically, it did not show a rapid lowering of cathode potential following application of the theoretical charge to reduce the inventory of MnO, as it did in runs 1 and 2. Rather, the cathode potential remained near -1.5V throughout the run. The cathode potential did drift lower towards the end of the run, but did not appear to reach lithium potential. This behavior suggests that some sodium metal may have formed at the cathode and introduced a parasitic and cyclic reaction with sodium metal oxidizing at the anode and reducing at the cathode. Run 3 was terminated after 42 A-hrs had been applied, which is nearly double the theoretical charge for the material loaded into cathode basket 3. While the post-test analysis of the product from run 3 showed substantial reduction of MnO, only 2.4% of the zirconium was found in the metal phase.

In light of the consequences of the observations in this study to the treatment of degraded EBR-II fuel, a substantial electrolytic reduction of zirconium oxide would not be expected. However, it is not clear from this study whether the presence of ZrO_2 would interfere with the electrolytic reduction of UO_2. Certainly, the presence of ZrO_2 mixed with uranium oxide would introduce some electrical resistance to a cathode material bed. Yet, run 2 in this study showed the MnO surrogate to still be substantially reduced to metal in spite of the presence of ZrO_2.

The presence of sodium oxide could interfere with uranium oxide reduction. While the addition of sodium oxide did not appear to significantly interfere with MnO reduction in the subject study, the electrolytic reduction response in run 3 did not reach the necessary lithium reduction potential to convert uranium oxide to metal. If run 3 did exhibit a parasitic and cyclic reaction of sodium metal formation at the cathode and oxidation at the anode, and the cyclic sodium reaction precluded lithium metal formation, then uranium reduction would not be expected. Additional experimental studies are needed to further investigate the direct impact of sodium oxide on electrolytic reduction of uranium oxide.

V. SUMMARY AND CONCLUSIONS

A series of three electrolytic reduction runs was performed at bench scale to assess the behavior of zirconium oxide and sodium oxide in LiCl – 1 wt% Li_2O at 650 °C using MnO as a surrogate for UO_2. In the absence of zirconium or sodium oxide, the electrolytic reduction of MnO showed nearly complete conversion to metal. The electrolytic reduction of a blend of MnO-ZrO_2 in LiCl – 1 wt% Li_2O showed substantial reduction of manganese, but only 8.5% of the zirconium was found in the metal phase. The electrolytic reduction of the same blend of MnO-ZrO_2 in LiCl – 1 wt% Li_2O – 6.2 wt% Na_2O showed substantial reduction of manganese, but zirconium reduction was even less at 2.4%.

This study concluded that ZrO_2 cannot be substantially reduced to metal in an electrolytic reduction system with LiCl – 1 wt% Li_2O at 650 °C due to the perceived preferential formation of lithium zirconate. This study also identified a possible interference that sodium oxide may have on the same system by introducing a parasitic and cyclic reaction of dissolved sodium metal between oxidation at the anode and reduction at the cathode. When applied to oxidized sodium-bonded EBR-II fuel (e.g., U-10Zr), the prescribed electrolytic reduction system would not be expected to substantially reduce zirconium oxide, and the accumulation of sodium in the electrolyte could interfere with the reduction of uranium oxide, or at least render it less efficient.

ACKNOWLEDGMENTS

This work was supported by the U.S. Department of Energy (DOE), Office of Nuclear Energy, under DOE Idaho Operations Office contract DE-AC07-05ID14517.

REFERENCES

1. BOARD OF CHEMICAL SCIENCES AND TECHNOLOGY, NATIONAL RESEARCH COUNCIL, Electrometallurgical Techniques for DOE Spent Fuel Treatment – Final Report, National Academies Press, Washington, D. C. (2000).
2. K. M. GOFF, J. C. WASS, K. C. MARSDEN, and G. M. TESKE, "Electrochemical Processing of Used Nuclear Fuel," *Nuclear Engineering and Technology*, **43**, *4*, 335 (2011).
3. K. GOURISHANKAR, L. REDEY, and M. WILLIAMSON, *Light Metals 2002*, p. 1075, W. SCHNEIDER, Ed., The Minerals, Metals & Materials Society, Warrendale, Pennsylvania (2002).
4. S. D. HERRMANN and S. X. LI, "Separation and Recovery of Uranium Metal from Spent Light Water Reactor Fuel via Electrolytic Reduction and Electrorefining," *Nuclear Technology*, **171**, 247 (2010).
5. G. F. BRUNZIE, T. R. JOHNSON, and R. K. STEUNENBERG, "Selective Dissolution of Uranium from Uranium-Uranium Oxide Mixtures by Bromine-Ethyl Acetate," *Analytical Chemistry*, **33**, *8*, 1005 (1961).
6. A. W. ASHBROOK, "The Determination of Uranium Metal in Products from the Reduction of Uranium Oxides with Magnesium," *Analyst*, **87**, 751 (1962).
7. *HSC Chemistry*, version 7.1, Outotec, Finland (2013).
8. W. PARK, J. M. HUR, E. Y. CHOI, and J. K. KIM, "Loss of Li_2O Caused by ZrO_2 During the Electrochemical Reduction of ZrO_2 in Li_2O-LiCl Molten Salt," *J. Korean Radioact. Waste Soc.*, **10**, *4*, 229 (2012).